

BENCHMARK SIMULATIONS OF CASE 4: DAYTIME CONVECTIVE DEVELOPMENT OVER LAND

Wojciech W. Grabowski*
NCAR[†], Boulder, Colorado

This document presents modeling strategy and preliminary results from an ensemble of simulation of the WG4 Case 4 of daytime convective development over land. The case is based on observations collected in the TRMM/LBA field project in Rondonia, Brazil. The simulations start from the early morning sounding and are driven primarily by increasing surface latent and sensible heat fluxes. Results are presented from a set of 3D simulations which start with high spatial resolution and relatively small computational domain (LES-type) and that apply a remapping procedure to move toward a setup with lower spatial resolution and larger computational domain, appropriate for deep convection.

1. ENSEMBLE OF BENCHMARK SIMULATIONS

The benchmark simulations are performed in the following manner, see Figs. 1, 2, and 3. We start with an LES-type setup with high spatial resolution (50 and 25 m horizontal and vertical grid spacing, respectively) with computational domain of $128 \times 128 \times 161$ (simulation S1; S for Smaller domain) and $192 \times 192 \times 161$ (simulation L1, L for larger domain). The computational domain, 6.4(S1)/9.6(L1) km in horizontal and 4 km in vertical, is large enough to represent development of convective boundary layer and shallow convective clouds in the first 3 hrs of the simulations.

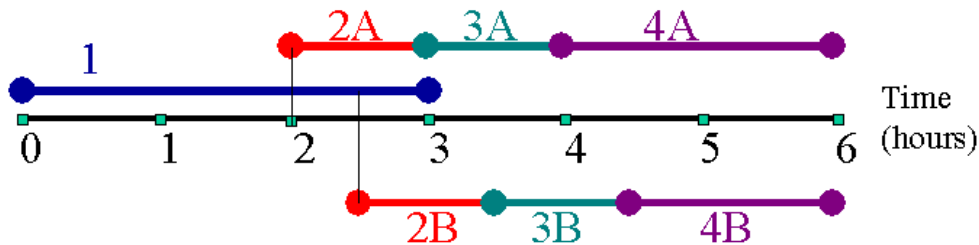


Figure 1: Timeline of the simulations performed.

To further capture development of convection, a larger horizontal domain (in both horizontal and vertical) is needed. The domain appropriate for deep convection, i.e., covering entire troposphere and extending several 10s of km in both horizontal directions, is reached by performing a remapping procedure three times, where higher-resolution fields at a given time are appropriately averaged to provide lower spatial resolution data needed to restart the model using larger computational domain. The fact that the model applies periodic lateral boundaries is essential. The procedure to create lower-resolution larger-domain fields is as follows. In the horizontal, the original higher-resolution fields are averaged over neighboring points to obtain fields in a horizontal domain that is four times larger, covered by the same number of gridpoints and using a horizontal grid spacing that is twice as large. Because of a particular realization of periodic lateral boundary conditions in EULAG, the remapping scheme produces 4 slightly different copies of lower horizontal resolution data in 4 quarters of the larger horizontal domain (cf. Fig. 2). In the vertical, the remapping from higher to lower resolution involves a similar averaging scheme as in the horizontal direction. Obviously, this is only possible in the part of the lower-resolution domain which covers the original higher-resolution domain. Model fields are taken from the initial sounding in the extended part of the vertical domain (cf. Fig. 3).

The remapping procedure is applied first at 2.0 and 2.5 hrs to start four sets of simulations (S2A and S2B starting from S1 and L2A and L2B starting from L1, cf. Fig. 1). These simulations apply horizontal and vertical grid spacing of 100 and 50 m, respectively. Each of these simulations is advanced 1 hour and the

* *Corresponding author address:* Dr. Wojciech W. Grabowski NCAR, PO Box 3000, Boulder, CO 80307; e-mail: grabow@ncar.ucar.edu.

[†] NCAR is sponsored by the National Science Foundation.

remapping procedure is repeated. Next the set of 4 simulations (S3A and S3B starting from S2A and S2B, respectively; L3A and L3B starting from L2A and L2B) apply horizontal and vertical grid spacing of 200 and 100 m, respectively. These simulations are again advanced by 1 hr and a final remapping is performed, only in the horizontal. The final set of simulations (S4A and L4A starting at 4 hrs, S4B and L4B starting at 4.5 hrs) is performed up to $t=6$ hrs. All simulations apply a 3-sec time step, except for later stages of simulations S1 and L1 (between 2 and 3 hrs) which require a 2-sec time step for numerical stability. Simulation details are summarized in Table 1.

2. EXAMPLE OF RESULTS

Figures 4 and 5 show evolutions of cloud fraction and height of the center of mass of the cloud field derived from ensemble of simulations, separated into sets S (Fig. 4) and L (Fig. 5). The evolution of cloud fraction shows considerable scatter among the simulations. It not possible to distinguish whether the scatter comes from inherently stochastic nature of this problem (i.e., different realizations are characterized by different cloud fractions as the depth of the cloud field increases) or if cloud fractions are strongly affected by the remapping procedure. In general, cloud fractions increase quite rapidly between hour 2 and 3 and tend to stay in the range 0.1-0.4 up to hour 5. The increase of cloud fraction in the final hour of simulation is likely associated with development of upper-tropospheric stratiform outflow anvil clouds associated with deep convection. The evolution of the center of mass of the cloud field shows less scatter, especially in the larger domain case, as one might expect. The center of mass raises steadily from about 0.5 km at 2 hrs to about 7 km at the end of simulations.

Figure 6 and 7 show evolutions of the surface precipitation rate, again separated into sets S and L. As the figures show, an ensemble of simulations is needed to estimate evolution of the mean surface precipitation rate due to stochastic nature of convection and rather small domain size from the dep convection point of view. The set of simulations performed is probably not large enough to obtain an accurate estimate of the surface precipitation, especially prior to $t=4$ hrs, when horizontal extent of the domain is rather small. However, the overall evolution of the mean surface precipitation rate shows that the values of about 0.01 mm/day are reached at about 3 hours of simulation and that the relatively steady mean rate of about 1 mm/day occurs after 5 hrs.

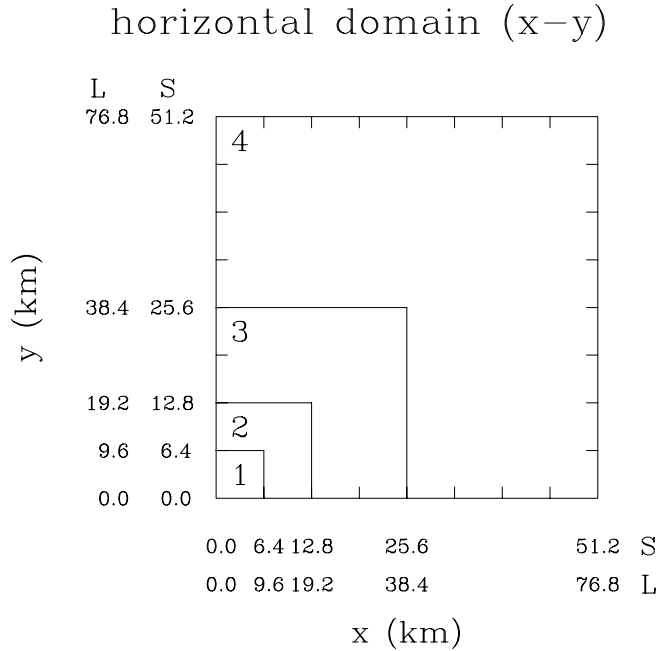


Figure 2: Increase of the horizontal domain size in the simulations.

vertical domain (x-z)

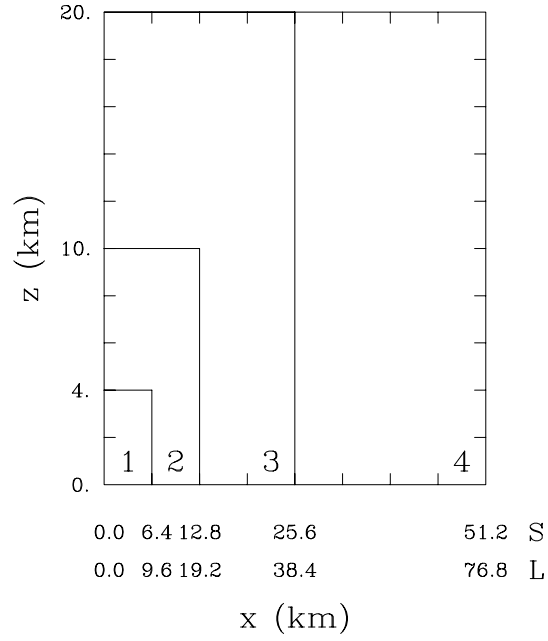


Figure 3: Increase of the domain size in the x-z plane.

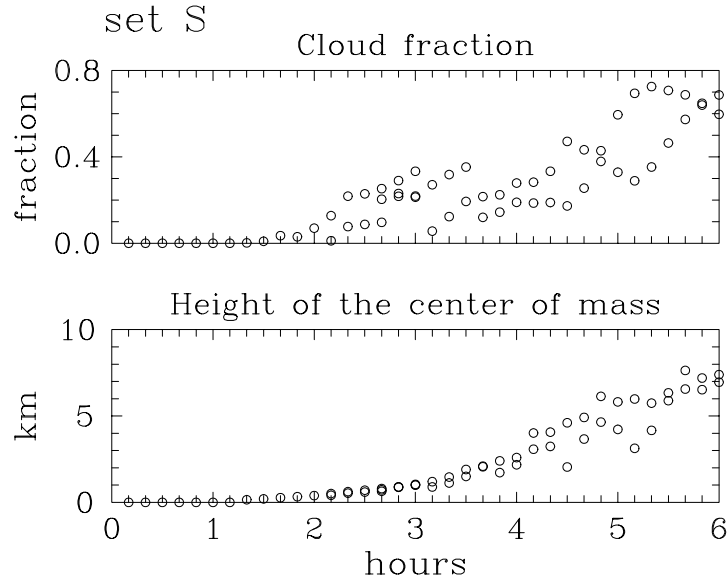


Figure 4: Evolution of the cloud fraction and height of the center of mass of the cloud field for the set S.

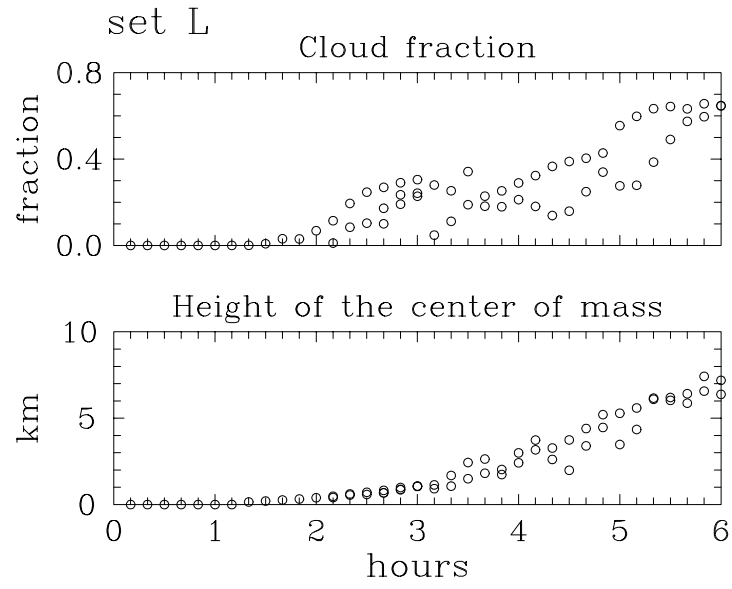


Figure 5: As Fig. 4, but for the set L.

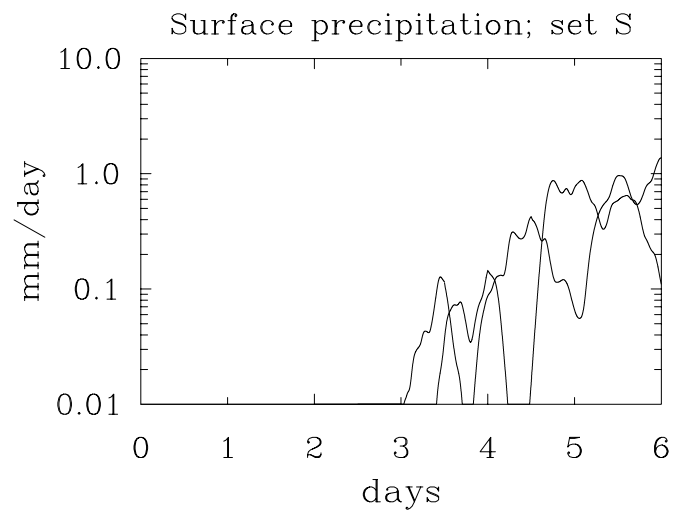


Figure 6: Evolution of the domain-averaged surface precipitation rate for the set S.

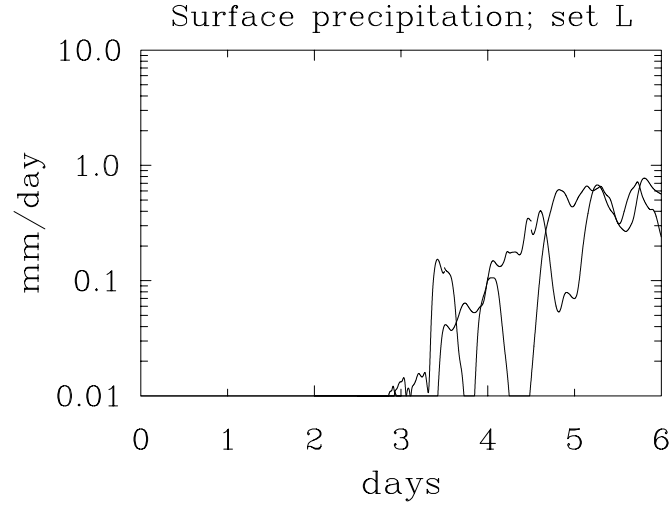


Figure 7: As Fig. 6, but for the set L.

List of simulations performed. The first column identifies the experiment. The second column gives horizontal grid spacing and the third column shows the horizontal extent of the domain. The fourth, fifth, and sixth columns show the vertical grid spacing, number of point in the vertical, and the vertical extent of the domain. The last three columns show starting and ending time of each simulations, and identify the simulation used to obtain the initial fields through the remapping procedure described in text.

	simulation code	dx,dy [m]	L_x [km]	dz [m]	nz	L_z [km]	start time [hr]	end time [hr]	started from
horizontal domain of 128 x 128, set S	S1	50	6.4	25	161	4.0	0.0	3.0	
	S2A	100	12.8	50	201	10.0	2.0	3.0	S1
	S2B	100	12.8	50	201	10.0	2.5	3.5	S1
	S3A	200	25.6	100	201	20.0	3.0	4.0	S2A
	S3B	200	25.6	100	201	20.0	3.5	4.5	S2B
	S4A	400	51.2	100	201	20.0	4.0	6.0	S3A
	S4B	400	51.2	100	201	20.0	4.5	6.0	S3B
horizontal domain of 192 x 192, set L	L1	50	9.6	25	161	4.0	0.0	3.0	
	L2A	100	19.2	50	201	10.0	2.0	3.0	L1
	L2B	100	19.2	50	201	10.0	2.5	3.5	L1
	L3A	200	38.4	100	201	20.0	3.0	4.0	L2A
	L3B	200	38.4	100	201	20.0	3.5	4.5	L2B
	L4A	400	76.8	100	201	20.0	4.0	6.0	L3A
	L4B	400	76.8	100	201	20.0	4.5	6.0	L3B

Figure 8: TABLE 1.